Differential quantal release of histamine and 5-hydroxytryptamine from mast cells of vesicular monoamine transporter 2 knockout mice

Eric R. Travis*, Yan-Min Wang†, Darren J. Michael*, Marc G. Caron†, and R. Mark Wightman*‡

*Department of Chemistry, University of North Carolina, Chapel Hill, NC 27599; and †Howard Hughes Medical Institute, Department of Cell Biology, Duke University Medical Center, Durham, NC 27710

Edited by Tomas Hökfelt, Karolinska Institute, Stockholm, Sweden, and approved November 11, 1999 (received for review July 26, 1999)

The recent availability of mice lacking the neuronal form of the vesicular monoamine transporter 2 (VMAT2) affords the opportunity to study its roles in storage and release. Carbon fiber microelectrodes were used to measure individual secretory events of histamine and 5-hydroxytryptamine (5-HT) from VMAT2-expressing mast cells as a model system for quantal release. VMAT2 is indispensable for monoamine storage because mast cells from homozygous (VMAT2$^{-/-}$) mice, while undergoing granule-cell fusion, do not release monoamines. Cells from heterozygous animals (VMAT2$^{+/-}$) secrete lower amounts of monoamine per granule than cells from wild-type controls. Investigation of corelease of histamine and 5-HT from granules in VMAT2$^{+/-}$ cells revealed 5-HT quantal size was reduced more than that of histamine. Thus, although vesicular transport is the limiting factor determining quantal size of 5-HT and histamine release, intragranular association with the heparin matrix also plays a significant role.

Vesicular monoamine transporters (VMATs) are proteins that transport monoamines from the cytoplasm into secretory vesicles (1–3). Along with monoamine synthesis and vesicular storage mechanisms, the transporter plays a central role in determining the amount of monoamine packaged in a vesicle to be available for subsequent quantal release by exocytosis (4). Thus, determining the relative role of these mechanisms is necessary to understand the regulation of chemical communication.

To investigate the importance of vesicular transport on monoamine release, we examined individual exocytotic release events of histamine and 5-hydroxytryptamine (5-HT) from mast cells isolated from VMAT2 knockout mice (5). Genetic deletion of the gene encoding VMAT2 enabled examination of release from individual vesicles in which transport was eliminated. Heterozygous (VMAT2$^{+/-}$) mice provided a situation where the number of transporters expressed was approximately halved, reducing the capacity for transport in comparison to cells from wild-type mice. In addition, we have compared results from the heterozygous cells with release from wild-type cells incubated with the VMAT2 selective inhibitor tetrabenazine (TBZ).

Mast cells have been used successfully as a model system to study both the role of Ca^{2+} in exocytosis (6) and the regulation of transmitter release during exocytosis (7). In that work they allowed analysis of exocytotic release characteristics of two different monoamines that are stored in the same vesicle but have different physical chemistries. The vesicular storage of histamine and 5-HT is promoted by their association with the highly negatively charged heparin matrix. The matrix in mast cell secretory granules has properties of a polyanionic hydrogel (8), and release of monoamines after granule-cell fusion appears to be driven by a cation-exchange process involving this matrix (9, 10). Because the nature of the association of the two monoamines with the heparin proteoglycan is quite different, this interaction can profoundly affect kinetics and extent of postfusion release (11, 12).

Both histamine and 5-HT are amenable to electrochemical detection with unparalleled sensitivity and spatio-temporal resolution with carbon-fiber microelectrodes (13). Amperometry and cyclic voltammetry were used in this study along with microscopic observations to analyze quantal secretion from individual cells. The hypothesis that VMAT2 expression regulates quantal size (1, 14, 15) was tested for the two costored monoamines. The results demonstrate the absolute necessity of the transporter for proper vesicular storage and release and reveal that vesicular monoamine transport is an important determinant of quantal size in monoamine-secreting cells.

Materials and Methods

VMAT2 Knockout Mice. VMAT2 knockout mice were generated as described (5). Briefly, the mouse *VMAT2* gene was cloned from a 129/SvJ library. Appropriate gene fragments were used to make the knockout construct. After confirming homologous recombination, positive embryonic stem clones were microinjected into C57BL/6 blastocysts and transferred into pseudopregnant mice. After birth, chimeric males showing germ-line transmission were used to breed with wild-type C57BL/6 females to generate F_1 and F_2 mice for experimental analyses. Individual mouse genotyping was performed by using three PCR primers and/or a Southern probe.

Mast Cell Preparation. Mast cells were obtained by peritoneal lavage with 400 μl (1–2 days old) to 5 ml (adult) of pH 7.4 physiological buffer (150 mM NaCl/5 mM KCl/1.2 mM $MgCl_2$/5 mM glucose/10 mM Hepes/2 mM $CaCl_2$). Buffer was retrieved and centrifuged at 200 *g* to pellet the peritoneal cells. Cells were resuspended in culture media (DMEM/Ham's F-12, Life Technologies, Grand Island, NY), plated, and incubated at 37°C before analysis. Mast cells normally comprised 5–10% of the total number of peritoneal cells and were readily identified under phase-contrast optics.

VMAT2 Immunofluorescence. Mast cells were obtained as described above and enriched through antibody-aided flow cytometry. Cells were resuspended and incubated with FITC-conjugated anti-B220 mAb and phycoerythrin-conjugated anti-Mac-1 mAb (Caltag, Burlingame, CA) to label the B cell and macrophage populations, respectively. After washing, the cells were sorted through a flow cytometer (FACScan, Becton Dickinson) by using both color selection and size exclusion. The double-

This paper was submitted directly (Track II) to the PNAS office.

Abbreviations: VMAT2, vesicular monoamine transporter; FSCV, fast-scan cyclic voltammetry; 5-HT, 5-hydroxytryptamine; C_{max}, maximal concentration of monoamine during exocytotic spike; +/+, wild-type; +/−, heterozygote; −/−, homozygote; TBZ, tetrabenazine.

‡To whom reprint requests should be addressed at: Department of Chemistry, University of North Carolina, CB 3290 Venable Hall, Chapel Hill, NC 27599-3290. E-mail: rmw@unc.edu.

The publication costs of this article were defrayed in part by page charge payment. This article must therefore be hereby marked "*advertisement*" in accordance with 18 U.S.C. §1734 solely to indicate this fact.

negative cells (≈10% of the total cells) were collected for VMAT2 immunofluorescent staining. They were fixed with 3% paraformaldehyde and incubated with secondary antibody-matched serum to block nonspecific sites. A primary rabbit anti-VMAT2 polyclonal antiserum (gift of J. Haycock, Louisiana State University Medical Center, New Orleans) was applied, and FITC-conjugated goat-anti-rabbit IgG was used as a secondary antibody. The cells were stained with toluidine blue to elicit metachromatic reaction of heparin and viewed with phase-contrast and fluorescence microscopy.

Carbon Fiber Microelectrodes. Glass-encased carbon fiber disk microelectrodes were constructed as described (16). Electrodes were back-filled with a 4 M potassium acetate, 150 mM KCl solution. Electrodes were calibrated with 5 μM histamine and 1 μM 5-HT.

Single Cell Analysis. A room-temperature culture plate with adhering cells was rinsed and placed in buffer solution. On the stage of an inverted microscope (Axiovert 35, Zeiss), a piezoelectric micromanipulator (PCS-1000 Patch Clamp Manipulator, Burleigh Instruments, Fishers, NY) was used to position the microelectrode adjacent to an isolated mast cell. For amperometry experiments, microelectrodes were placed in direct contact with the plasma membrane. Microelectrodes were positioned 1 μm away from the cell surface for background-subtracted fast-scan cyclic voltammetry (FSCV) experiments (13). Release was induced with 10-sec pressure ejection (8 psi, Picospritzer, General Valve, Fairfield, NJ) of 0.5 μM calcium ionophore A23187 from a 10-μm inner diameter glass micropipette positioned 30–50 μm from the cell (16).

Electrochemistry: FSCV. FSCV measurements were made under computer control by using a potentiostat (EI-400, Cypress Systems, Lawrence, KS) in two-electrode mode. To enable simultaneous histamine and 5-HT detection (16), the electrode potential was scanned from a rest potential of +100 mV to +1,400 mV and back to +100 mV at 800 V/s (potentials referenced to sodium-saturated calomel electrode) and at a repetition rate of 30 Hz. Programs for data acquisition (17) were written in LABVIEW (National Instruments, Austin, TX). For FSCV spike detection and parameter analysis, locally written software was used to evaluate in parallel the current-time traces obtained by averaging data in the 100-mV window centered on peak oxidation potentials for histamine and 5-HT. Spike maximal amplitudes were converted to units of maximal concentration (C_{max}) based on postexperiment electrode calibrations. FSCV experiments and electrode calibrations were performed in a pH 7.4 Tris buffer (12.5 mM Tris·HCl/150 mM NaCl/4.2 mM KCl/1.4 mM $MgCl_2$/5.6 mM glucose/1.5 mM $CaCl_2$; ref. 16).

Electrochemistry: Constant Potential Amperometry. For amperometry measurements, a patch-clamp instrument (Axopatch 200B, Axon Instruments, Foster City, CA) was used in voltage clamp mode. At a potential of +650 mV versus sodium-saturated calomel electrode, microelectrode current was monitored (10-kHz low-pass filter) and digitized to videotape (PCM-2 A/D VCR Adaptor, Medical Systems, Greenvale, NY). At +650 mV, 5-HT is oxidized at the electrode but histamine is not. Amperometry experiments were performed in the Hepes buffer used for cell isolation.

Optical Imaging of Exocytosis. In some experiments, visualization of exocytosis was enhanced with 50 μg/ml ruthenium red, which avidly binds to heparin (18). Individual mast cells were stimulated via pressure ejection of A23187 and monitored through the microscope with a charge-coupled device camera. Ruthenium red was found to partition into mast cell heparin exposed to the cell surface after granule-cell fusion, enabling visualization of the exocytotic process in real time.

Reagents and Solutions. Histamine dihydrochloride, 5-HT hydrochloride, epinephrine (free base), toluidine blue, ruthenium red, and calcium ionophore A23187 were obtained from Sigma. TBZ was obtained from Fluka. All other compounds were obtained from Sigma and used as received, unless otherwise noted. A23187 stimulating solution was prepared by 1,000-fold dilution in physiological buffer of a stock solution in DMSO. Histamine and 5-HT solutions for electrode calibration were prepared by dilution in buffer of stock solutions in 0.1 M $HClO_4$. Solutions were prepared in doubly distilled deionized water and adjusted to pH 7.4 by addition of NaOH or HCl.

Results

Presence of VMAT2 in Murine Mast Cells. Immunofluorescence was used to check for expression of VMAT2 in mouse peritoneal mast cells, which were purified by using antibody-aided flow cytometry. Identity of mast cells was confirmed by metachromatic staining of heparin with toluidine blue. Cells that stained positive with toluidine blue concurrently displayed VMAT2 immunofluorescence (see Fig. 6, which is published as supplementary material on the PNAS web site, www.pnas.org). Thus, VMAT2 expression is confirmed in the cells used for studies of exocytosis.

Absence of Monoamine Quantal Release from VMAT2$^{-/-}$ Mast Cells. To investigate the effects of VMAT2 absence on monoamine release, mast cells were obtained from newborn homozygous mice (VMAT2$^{-/-}$) as well as VMAT2$^{+/-}$ and wild-type (VMAT2$^{+/+}$) littermates. Newborn mast cells were approximately 8 μm in diameter, compared with the 10- to 12-μm diameter adult mast cells. With the microelectrode potential at +650 mV, amperometry allows temporally resolved measurement of quantal release of 5-HT without detection of histamine (16). Cells from VMAT2$^{+/+}$ and VMAT2$^{+/-}$ newborn mice exhibited 5-HT secretion when exposed to the calcium ionophore A23187 (Fig. 1). In contrast, none of the 53 stimulated cells examined from seven VMAT2$^{-/-}$ pups showed any current transients. Cyclic voltammetry was used to confirm that histamine also is released from wild-type and VMAT2$^{+/-}$ cells from pups, but not VMAT2$^{-/-}$ cells (see Fig. 7, which is published as supplementary material on the PNAS web site).

Visual Observation of Granule-Cell Fusion in VMAT2$^{-/-}$ Mast Cells. Visual monitoring of mast cell degranulation was used to evaluate the exocytotic competency of cells from newborn VMAT2$^{-/-}$ mice. Because of the relatively large size of mast cell secretory granules (0.7 μm mean diameter in adult cells), the morphological changes that occur at the cell membrane because of granule-cell fusion can be observed microscopically. Mast cells of all genotypes exhibited clear degranulation upon stimulation with A23187 in the presence of Ca^{2+}. Because mast cells from newborns are somewhat smaller and have less robust release characteristics compared with their adult counterparts, ruthenium red staining was used to enhance visualization of exocytosis (18). Pressure ejection of A23187 onto the cell evokes exocytosis that is observed as a progressive increase in cell surface staining caused by incorporation of the cationic red dye into discrete areas where polyanionic heparin is exposed to the outer surface by granular fusion (Fig. 2). The appearance of red punctate staining indicated a rapid succession of individual granule fusion events distributed over the entire cell surface, leading to a general disruption of the previously well-defined cell membrane. By this method, exocytosis was observed to occur in mast cells from newborns for all genotypes, including VMAT2$^{-/-}$ cells.

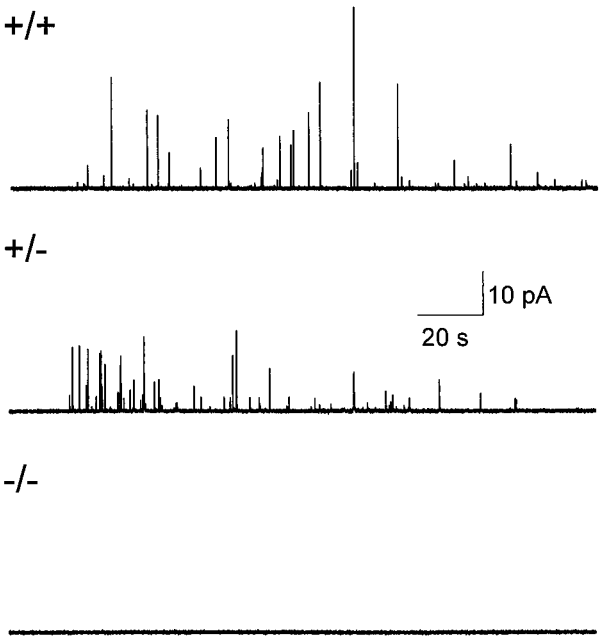

Fig. 1. Amperometric measurement of exocytosis from newborn VMAT2$^{+/+}$, VMAT2$^{+/-}$, and VMAT2$^{-/-}$ mast cells. Traces show secretory responses of calcium ionophore A23187-stimulated cells representative of each genotype as measured by amperometry (+650 mV vs. sodium-saturated calomel electrode).

Histamine and 5-HT Release from VMAT2$^{+/-}$ Mast Cells. The three-dimensional false-color plot in Fig. 3 shows a 20-sec segment of background-subtracted FSCV data obtained at an adult VMAT2$^{+/-}$ mast cell stimulated with A23187. The color plot (19) represents all of the current data as a function of electrode potential obtained during a series of repeated potential scans. As shown in the two-dimensional cyclic voltammogram (top of Fig. 3) taken from one of the transient current features in the data, each voltage scan (3.25 ms in duration) provides information on electroactive species present at the electrode surface. The voltammetric peak that occurs around +550 mV on the forward scan corresponds to 5-HT oxidation. The oxidative peak that occurs around +1,300 mV is caused by histamine. The additional peak often seen on the forward scan is a time-dependent wave resulting from a histamine product generated by prior voltage scans (16). If the voltammetric current is sampled on successive scans and averaged in the 100-mV peak oxidation potential

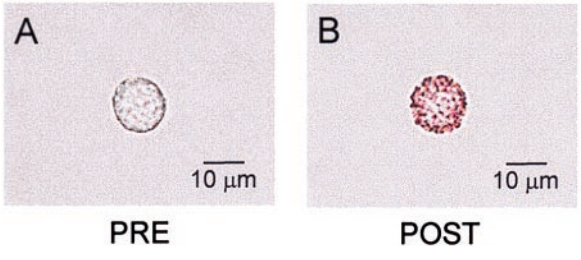

Fig. 2. Bright-field photomicrographs show degranulation of mouse peritoneal mast cell with visual enhancement by ruthenium red staining. A VMAT2$^{+/+}$ mast cell in 50 μg/ml of ruthenium red solution is shown before (*A*) and 5 min after (*B*) pressure ejection of A23187 solution onto the cell from a nearby stimulating pipette. Morphological changes in cell border and staining of heparin from individual fused granules clearly demonstrate exocytosis has occurred.

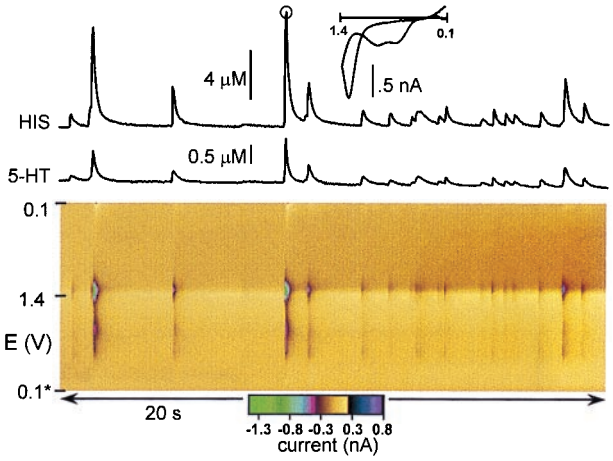

Fig. 3. FSCV measurement of cosecretion of histamine and 5-HT from A23187-stimulated VMAT2$^{+/-}$ mast cell. The upper (HIS) trace shows changes in histamine concentration over the 20-s interval by sampling current at +1,300 mV (reverse scan) on successive scans. The lower (5-HT) trace shows changes in 5-HT concentration obtained by sampling current at +550 mV vs. sodium-saturated calomel electrode (forward scan) on successive scans. The inset plot shows a single cyclic voltammogram taken at the peak time of the circled spike.

window for histamine, a current trace is obtained that tracks changes in histamine concentration (Fig. 3, upper trace). Similarly, a plot that follows 5-HT concentration changes may be constructed by averaging the current in the 100-mV oxidation potential window for 5-HT (Fig. 3, lower trace).

The representative VMAT2$^{+/-}$ cell in Fig. 3 exhibits corelease of histamine and 5-HT in response to stimulation. Similar data were obtained at VMAT2$^{+/+}$ cells. However, release concentrations differed between VMAT2$^{+/+}$ and VMAT2$^{+/-}$ cells. On average, VMAT2$^{+/-}$ cells exhibited histamine spike amplitudes (C_{max}s) that were 32% smaller and 5-HT spike amplitudes that were 57% smaller than those of the wild-type littermates (Fig. 4*A*). For some histamine spikes, corresponding 5-HT spikes were absent or lost in baseline noise. The time course of each release event was not significantly altered by VMAT2 expression as indicated by similar spike widths. For each temporally correlated secretion event, the resulting ratio of histamine to 5-HT for VMAT2$^{+/-}$ spikes was approximately double that of VMAT2$^{+/+}$ spikes (Fig. 4*A*). This difference in secreted amounts is also apparent in Fig. 4*B* where histamine C_{max} and 5-HT C_{max} are plotted for each secretion event and grouped by genotype. Though the scatterplots reveal that C_{max} ratios are heterogeneous, a linear correlation exists. The 2-fold difference in regression line slope between the two genotypes also reflects the difference in histamine/5-HT ratio.

At mast cells from both genotypes, some exocytotic events exhibit a small amplitude feature that precedes the main body of the concentration spike. This prespike feature, or "foot," is believed to correspond to detection of the flux of transmitter molecules through a fusion pore before complete expansion and release of vesicle content (20, 21). Well-resolved FSCV recordings of release during the foot (example shown in Fig. 5) show simultaneous histamine and 5-HT appearance. A cyclic voltammogram obtained during the spike phase further demonstrates that the species detected during the foot and spike are identical.

Effects of Long-Term Incubation with TBZ on Histamine and 5-HT Release. Monoamine release from mast cells of wild-type adult animals also was examined after incubation with TBZ, a VMAT2 selective inhibitor. No effects were seen on exocytotic release with incubations up to 1 hr with 10 μM TBZ. However, 24-hr

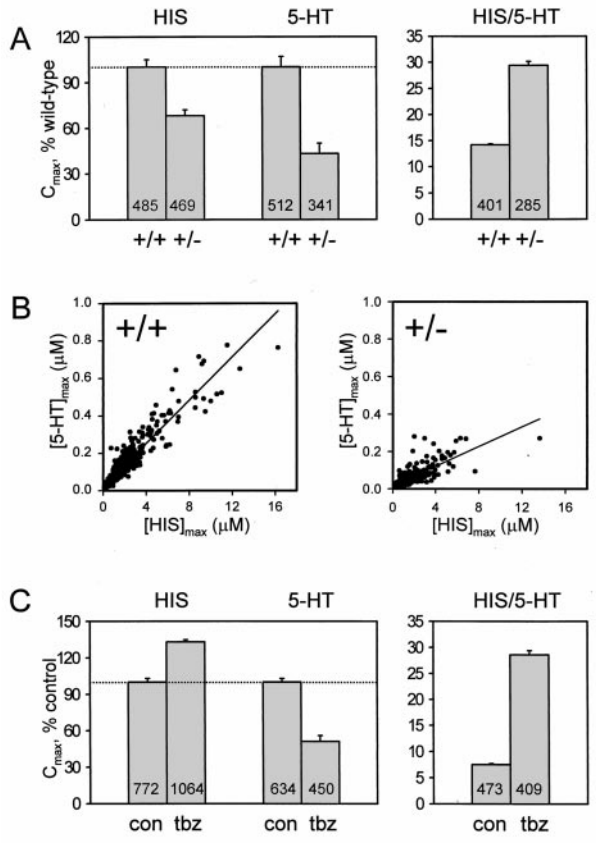

Fig. 4. Analysis of histamine and 5-HT concentration spike amplitudes observed by cyclic voltammetry during exocytosis at mast cells. (*A*) Effects of reduced VMAT2 expression on histamine and 5-HT FSCV spike amplitudes. (*Left*) A comparison of mean histamine and 5-HT spikes (C_{max})for secretion measured from VMAT2$^{+/+}$ (n = 13 cells of two mice) and VMAT2$^{+/-}$ (n = 12 cells of two mice) mast cells. Data are expressed as percent of wild-type response with the dashed line showing 100%. (*Right*) The mean ratio of histamine to 5-HT for simultaneously occurring spikes from the two genotypes. (*B*) Scatterplots of 5-HT C_{max} versus histamine C_{max} for temporally coincident secretory spikes measured at VMAT2$^{+/+}$ and VMAT2$^{+/-}$ mast cells. For VMAT2$^{+/+}$ cells (401 spikes from 13 cells of two mice), linear regression line has slope of 0.06 and correlation coefficient of 0.94. For VMAT2$^{+/-}$ data (285 spikes from 12 cells of two mice), the slope is 0.03 and correlation coefficient is 0.77. (*C*) Effects of inhibition of VMAT2 on histamine and 5-HT FSCV spike amplitudes. (*Left*) A comparison of mean histamine and 5-HT spike C_{max} for secretion from VMAT2$^{+/+}$ mast cells, both untreated (con, n = 10) and incubated with 10 μM TBZ for 24 hr (n = 11). Data are expressed as percent of control response with dashed lines showing 100%. (*Right*) Mean ratio of histamine C_{max} to 5-HT C_{max} for simultaneously occurring spikes of control and TBZ-treated cells. Error bars are SEM. The number of spikes detected and analyzed under each condition is shown on the bar.

incubation with 10 μM TBZ profoundly affected the amplitude of individual 5-HT secretory spikes measured by cyclic voltammetry (Fig. 4*C*). The average 5-HT concentration spike amplitude (C_{max}) for TBZ-treated cells was 51% of average 5-HT C_{max} for control cells of the same animals. Average histamine C_{max}, on the other hand, was found to be nearly 33% greater than control. For temporally matched histamine and 5-HT spikes, the histamine to 5-HT C_{max} ratio was 7.5 for control cells and 28.6 for TBZ-treated cells. Thus, pharmacological inhibition of VMAT2 also causes a dramatic increase in the histamine/5-HT ratio.

Discussion

The results of this study at the level of individual release events provide confirmation that VMAT2 is essential for granular

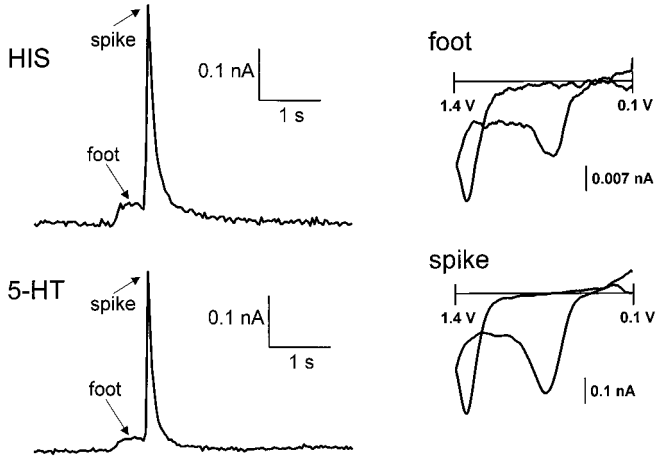

Fig. 5. FSCV detection of histamine and 5-HT released through fusion pore of VMAT2$^{+/+}$ mast cell. Electrochemical current sampled at peak oxidation potentials for both histamine (*Upper Left*) and 5-HT (*Lower Left*) during an individual exocytotic event exhibit the presence of a foot. Concentrations measured at the electrode during the foot were 0.03 and 0.31 μM for 5-HT and histamine, respectively. In contrast, the spike peak concentrations were 0.48 and 4.38 for 5-HT and histamine, respectively. (*Right*) Cyclic voltammograms obtained during the foot and at the spike maximum are shown. Their similarity clearly shows that the same species are released during the two phases of exocytosis.

monoamine accumulation and, thus, its subsequent release. Although VMAT2$^{-/-}$ mice only survive a few days, mast cells could be obtained from newborn animals and their wild-type and VMAT2$^{+/-}$ littermates, enabling their release characteristics to be compared. The electrochemical techniques allowed simultaneous measurement of 5-HT and histamine secretion. The temporal correspondence of monoamine concentration spikes during exocytosis from cells isolated from VMAT2$^{+/+}$ and VMAT2$^{+/-}$ mice indicates that histamine and 5-HT are coreleased from the same secretory granule as shown previously in rat peritoneal mast cells (16). The two monoamines also were found to be coreleased during the initial formation of the fusion pore that precedes the primary secretory events from both VMAT2$^{+/+}$ and VMAT2$^{+/-}$ mast cells. In dramatic contrast, mast cells without VMAT2 do not release either amine during exocytosis. Exocytosis at mast cells from all three types of mice was readily visualized in the presence of ruthenium red because of its accumulation in polyanionic heparin accumulated on the cell surface.

Two subtypes of monoamine transporter (VMAT1 and VMAT2) have been cloned and characterized (22–25). The mutant mice used in this work lack the neuronal isoform VMAT2 (5, 15, 26). VMAT2$^{+/-}$ mice exhibit reduced levels of brain monoamines whereas VMAT2$^{-/-}$ mice are almost completely devoid of brain monoamines (5, 15). Depolarization induced monoamine release from brain measured *in vivo* or from cell cultures is eliminated in the homozygous animals. Release from cultured VMAT2$^{+/-}$ neurons is half of that found in VMAT2$^{+/+}$ cells (15). This work provides additional information in that it allows an assessment at the level of individual excocytotic events as to how alterations in VMAT2 expression affect monoamine release. VMAT2 has been postulated to be the isoform in mast cells (27, 28) because the affinity of VMAT2 for histamine (K_M = 3.06 μM) is much higher than that of VMAT1 (K_M = 436 μM) (29). Our immunocytochemical result confirms this hypothesis. The absence of either histamine or 5-HT release from VMAT2$^{-/-}$ cells shows that other transporters, including VMAT1, are unable to replace, in the homozygous animals, the role normally played by VMAT2.

Previously, it has been hypothesized that VMATs could influence quantal release by a change in quantal size or a change in quantal number (1, 14). VMAT2 control over quantal size implies that kinetics of monoamine transport into the vesicle determine the amount available for release. A change in quantal number would imply VMAT2 involvement in regulation of vesicle biogenesis or recruitment. The present work establishes that VMAT2 expression exerts its principal influence on quantal size. Conversely, overexpression of VMAT2 (15) or the vesicular acetylcholine transporter (30) both result in several-fold increases in quantal size. However, quantitative examination of the results from $VMAT2^{+/+}$ and $VMAT2^{+/-}$ mast cells from adult animals reveals that storage of 5-HT and histamine is regulated differentially. 5-HT released from $VMAT2^{+/-}$ mast cell granules is 43% of that from wild-type cells whereas histamine released from $VMAT2^{+/-}$ cells is 68% of that from wild-type cells. Thus, in addition to VMAT2, other factors must play an important role in regulating monoamine storage.

In the heterozygous animal, differences in substrate availability could be the origin of the observed difference in relative secretion. Indeed, because histamine can inhibit 5-HT uptake (27), an excess of this amine would lead to a decrease in released 5-HT. Another factor affecting storage of both monoamines in mast cell granules is the association of histamine and 5-HT with the granular matrix comprised of negatively charged heparin and basic protein. The granular association is quite strong, leading to a half-life of histamine in mast cells of greater than 20 days (31). During exocytosis, the matrix dissociates upon encountering the higher pH and lower osmolarity of the extracellular fluid (32). Histamine is more strongly associated with the heparin matrix (33) because, at the intragranular pH of 5.8 (34), about half of the histamine is diprotonated ($pK_{a2} = 5.9$) whereas the majority of the 5-HT is monoprotonated ($pK_{a2} = 4.9$). Prior studies of quantal release from mast cells have revealed that this differential association of histamine and 5-HT with the granule matrix profoundly affects the kinetics and extent of exocytotic release (12).

A mechanism that accounts for VMAT2 transport, storage and release is given in the following scheme:

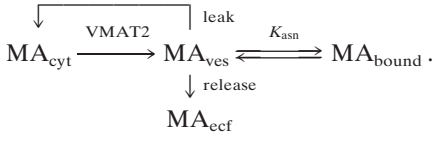

VMAT2 is responsible for transporting cytoplasmic monoamine (MA_{cyt}) to the vesicle interior whereas a leakage mechanism (leak) contributes to its return to the cytoplasm (4). Normally, the soluble portion of monoamine in the vesicle (MA_{ves}) exists in an equilibrium (defined by K_{asn}) with monoamine that is bound to the granule matrix (MA_{bound}). When exocytosis occurs, MA_{ves} can leave the granule and the carbon-fiber microelectrode detects it in the extracellular fluid (MA_{ecf}). Thus, MA_{ves} is the source of the "foot" events that occur immediately upon formation of the fusion pore (20). Pore formation is followed by granular swelling that decreases K_{asn}, increasing MA_{ves} and leading to the concentration spikes observed electrochemically. As a result of the stronger association of histamine with the matrix when compared with 5-HT, the relative amount of releasable histamine under storage conditions is less than that of 5-HT. Thus, even though they are in the same granule, 5-HT has more opportunity to leak into the cytoplasm, which places a stronger demand on VMAT2 to maintain its stored amount. The net result is that 5-HT quantal size will be more sensitive to functional VMAT2 levels than histamine.

To test this scheme under conditions where substrate availability should not be an issue, VMAT2 in mast cells from wild-type mice was pharmacologically inhibited. Prolonged incubation with TBZ was required for a measurable effect, indicating that, in spite of the weaker association of 5-HT with the intragranular matrix, matrix dissociation kinetics and leakage are quite slow in the granule during storage. In contrast, the egress of monoamines from small, clear neuronal vesicles, where intravesicular association is less likely, occurs in a few minutes after VMAT2 inhibition (35). However, similar to the effects of reduction in VMAT2 expression on mast cell storage, inhibition of the transporter leads to differential changes in granular monoamine release. In this case, only the amount of 5-HT release was diminished whereas histamine spike amplitude actually increased. Because substrates were not added and the content could not change, the only mechanism whereby this effect could arise would be from 5-HT granular leakage during TBZ incubation causing a change in K_{asn}, thus allowing more bound histamine to become soluble in the vesicle. Indeed, granule swelling indicative of reduced association is observed upon egress of 5-HT from the granule (10). 5-HT release could be further modulated by the increased cytoplasmic histamine because it also can inhibit VMAT2-mediated 5-HT transport (25). Thus, with both reduced VMAT2 number and its pharmacological inhibition, we find that 5-HT is depleted to a greater degree than histamine.

The present results show that differential regulation of chemical messenger storage in the same vesicle can occur if a strongly associating matrix is present, a fact not previously appreciated. Therefore, in addition to the fundamental importance of VMAT2 transport, polyanionic storage matrices that promote intravesicular storage also play an important role in maintaining chemical levels in vesicles and the amount released during chemical communication. These findings have direct relevance for neurotransmitters stored in dense core vesicles where protein-small molecule association also can occur. However, as shown in this work, even when intravesicular association promotes storage, VMATs are essential for transport of monoamines into their storage location. Because the monoamines transported by VMAT2 in neurons regulate mood and emotion, alterations in functional VMAT2 could have significant behavioral effects by modulation of neuronal communication.

This research was supported by grants from the National Institutes of Health (DA 10900 and NS 38879 to R.M.W. and NS 09930 to M.G.C.) and a Bristol-Myers Squibb Unrestricted Research Award (to M.G.C.).

1. Henry, J. P., Sagne, C., Bedet, C. & Gasnier, B. (1998) *Neurochem. Int.* **32,** 227–246.
2. Varoqui, H. & Erickson, J. D. (1997) *Mol. Neurobiol.* **15,** 165–191.
3. Schuldiner, S. (1994) *J. Neurochem.* **62,** 2067–2078.
4. Williams, J. (1997) *Neuron* **18,** 683–686.
5. Wang, Y. M., Gainetdinov, R. R., Fumagalli, F., Xu, F., Jones, S. R., Bock, C. B., Miller, G. W., Wightman, R. M. & Caron, M. G. (1997) *Neuron* **19,** 1285–1296.
6. Neher, E. (1998) *Neuron* **20,** 389–399.
7. Rahamimoff, R. & Fernandez, J. M. (1997) *Neuron* **18,** 17–27.
8. Curran, M. J. & Brodwick, M. S. (1991) *J. Gen. Physiol.* **98,** 771–790.
9. Uvnas, B. & Aborg, C.-H. (1989) *News Physiol. Sci.* **4,** 68–71.
10. Marszalek, P. E., Farrell, B., Verdugo, P. & Fernandez, J. M. (1997) *Biophys. J.* **73,** 1169–1183.
11. Pihel, K., Travis, E. R., Borges, R. & Wightman, R. M. (1996) *Biophys. J.* **71,** 1633–1640.
12. Pihel, K., Hsieh, S. C., Jorgenson, J. W. & Wightman, R. M. (1998) *Biochemistry* **37,** 1046–1052.
13. Travis, E. R. & Wightman, R. M. (1998) *Annu. Rev. Biophys. Biomol. Struct.* **27,** 77–103.
14. Reimer, R. J., Fon, E. A. & Edwards, R. H. (1998) *Curr. Opin. Neurobiol.* **8,** 405–412.

15. Fon, E. A., Pothos, E. N., Sun, B. C., Killeen, N., Sulzer, D. & Edwards, R. H. (1997) *Neuron* **19,** 1271–1283.
16. Pihel, K., Hsieh, S. C., Jorgenson, J. W. & Wightman, R. M. (1995) *Anal. Chem.* **67,** 4514–4521.
17. Michael, D. J., Joseph, J. D., Kilpatrick, M. R., Travis E. R. & Wightman, R. M. (1999) *Anal. Chem.* **71,** 3941–3947.
18. Lagunoff, D. (1972) *J. Histochem. Cytochem.* **20,** 938–944.
19. Michael, D., Travis, E. R. & Wightman, R. M. (1998) *Anal. Chem.* **70,** 586A–592A.
20. Alvarez de Toledo, G., Fernandez-Chacon, R. & Fernandez, J. M. (1993) *Nature (London)* **363,** 554–558.
21. Wightman, R. M., Schroeder, T. J., Finnegan, J. M., Ciolkowski, E. L. & Pihel, K. (1995) *Biophys. J.* **68,** 383–390.
22. Erickson, J. D., Schafer, M. H., Bonner, T. I., Eiden, L. E. & Weihe, E. (1996) *Proc. Natl. Acad. Sci. USA* **93,** 5166–5171.
23. Weihe, E., Schafer, M. H., Erickson, J. D. & Eiden, L. E. (1994) *J. Mol. Neurosci.* **5,** 149–164.
24. Peter, D., Liu, Y. J., Sternini, C., DeGiorgio, R., Brecha, N. & Edwards, R. H. (1995) *J. Neurosci.* **15,** 6179–6188.
25. Liu, Y. J., Peter, D., Merickel, A., Krantz, D., Finn, J. P. & Edwards, R. H. (1996) *Behav. Brain Res.* **73,** 51–58.
26. Takahashi, N., Miner, L. L., Sora, I., Ujike, H., Revay, R. S., Kostic, V., Jackson-Lewis, V., Przedborski, S. & Uhl, G. R. (1997) *Proc. Natl. Acad. Sci. USA* **94,** 9938–9943.
27. Merickel, A. & Edwards, R. H. (1995) *Neuropharmacology* **34,** 1543–1547.
28. Erickson, J. D., Eiden, L. E., Schafer, M. H. & Weihe, E. (1995) *J. Mol. Neurosci.* **6,** 277–287.
29. Peter, D., Jimenez, J., Liu, Y., Kim, J. & Edwards, R. H. (1994) *J. Biol. Chem.* **269,** 7231–7237.
30. Song, H. J., Ming, G. L., Fon, E., Bellocchio, E., Edwards, R. H. & Poo, M. M. (1997) *Neuron* **18,** 815–826.
31. Ludowyke, R. I. & Lagunoff, D. (1986) *Biochemistry* **25,** 6287–6293.
32. Wingren, U., Wasteson, A. & Enerback, L. (1983) *Int. Arch. Allergy Appl. Immunol.* **70,** 193–199.
33. Rabenstein, D. L., Bratt, P. & Peng, J. (1998) *Biochemistry* **37,** 14121–14127.
34. Rabenstein, D. L., Ludowyke, R. & Lagunoff, D. (1987) *Biochemistry* **26,** 6923–6926.
35. Floor, E. Leventhal, P. S., Wang, Y., Meng, L. & Chen, W. (1995) *J. Neurochem.* **64,** 689–699.